Appl Phys B (2010) 98: 759–765
DOI 10.1007/s00340-009-3808-1

Applied Physics B
Lasers and Optics

Instantaneous frequency measurement applied to semiconductor laser relaxation oscillations

D.M. Kane · C.J. McMahon

Received: 16 July 2009 / Revised version: 7 October 2009 / Published online: 5 November 2009

Abstract The frequency of relaxation oscillations in the output power of lasers, particularly semiconductor lasers, is an important parameter which can be used to inform other fundamental laser variables, for comparison with expected theory, and to show the effect of external influences, such as optical feedback, by a change in value. Thus, precision measurement of the relaxation frequency is important. Instantaneous frequency measurement algorithms are applied to experimental semiconductor laser relaxation-oscillation signals to determine whether reliable values can be extracted, for an extended range of injection current, as compared to direct measurement and fast Fourier transform techniques. Improvement is achieved but, more importantly, the technique clearly shows when other oscillations, such as those due to packaging, connectorization and power supply, dominate the oscillatory component of the output power, at low injection currents. The work further supports the finding that only mid-range injection currents can be used for reliable precision relaxation oscillation frequency measurement.

PACS 42.55.Px · 42.60.Rn

1 Introduction

Relaxation oscillations (ROs) in output power are a characteristic of many classes of lasers. In particular, for semiconductor lasers, the angular frequency of the relaxation oscillation, ω_{RO}, is predicted to scale as the square root of the injection current above threshold as given in (1) [1]. It takes values in the gigahertz to tens of gigahertz frequency range, at injection currents giving useful output powers.

$$\omega_{\mathrm{RO}} \approx \sqrt{\left(\frac{\mathrm{d}G}{\mathrm{d}n}\right)\frac{I_{\mathrm{in}} - I_{\mathrm{th}}}{eV}\frac{1}{\tau_{\mathrm{ph}}}}. \tag{1}$$

Here G is the normalized gain, n is the carrier density, I_{in} is the injection current, I_{th} is the threshold current, τ_{p} is the photon lifetime and V is the volume of the active layer. Knowledge of the relaxation oscillation frequency of a laser, therefore, has value in informing a number of fundamental laser variables [2]. In optical communications, highly damped semiconductor lasers are employed as the source of choice. As a consequence, it can be very difficult to measure the relaxation oscillation frequency.

A method based on time averaging about 1000 relaxation oscillation events, captured in real time, has been developed [3]. It has been used to show agreement with the expected theoretical dependency on injection current above threshold described by (1). However, it has been necessary to restrict the range of injection currents used in the fit to a mid range—starting from about 5 mA above threshold and finishing about 20 mA above threshold. Trends in the measured relaxation oscillation frequency at near-threshold and high injection currents are found to be inconsistent with the expected frequency–current relationship and require further investigation to determine whether the theory of (1) no longer applies, or whether it is just not possible to measure the relaxation oscillation frequency due to reduced signal-to-noise and/or the heavy damping. For injection currents of more than 20 mA above threshold the relaxation oscillations are so heavily damped that less than one full oscillation, of relatively small amplitude, may be captured. At injection currents close to threshold the relaxation oscillation

D.M. Kane (✉) · C.J. McMahon
Department of Physics, Macquarie University, Sydney, NSW 2109, Australia
e-mail: debkane@science.mq.edu.au
Fax: +61-2-98508115

events are also small in amplitude, compared to those for mid-range currents, and may be masked by noise and possibly other sources of oscillation.

Recently, it has been demonstrated that precision relaxation oscillation frequency (ROF) measurement, as a function of injection current, leads to the most precise value of the laser threshold injection current of a semiconductor laser reported to date [4]. Additionally, this measure of the threshold current is based on fundamental laser physics—the injection current at which a relaxation frequency of zero occurs, as extrapolated from ROF measurements at higher injection currents. An order of magnitude improvement in precision is achieved by this method [4], as compared to the second-derivative method for determining laser threshold current. The latter is the most precise method for estimating threshold current of a semiconductor laser defined in the Bellcore standard [5]. This use of precision ROF measurements provides a further motivation for extending the range of injection currents over which meaningful ROF measurements can be made.

In this work we test whether the method of instantaneous frequency measurement (IFM) [6–8] can be used to extract reliable ROF values from experimental relaxation oscillation frequency signals. This has been done successfully. Further, we test whether IFM allows reliable ROF values to be obtained for an extended range of injection currents, as compared to previous methods used. Modest improvements are obtained.

2 Semiconductor laser relaxation oscillations

The relaxation oscillation data used in this study has been reported previously [3]. The data is re-analyzed to extract an instantaneous frequency measurement. The semiconductor laser was an STC (LT50-03U) multiple quantum well device, operating at 850 nm. The temperature of the device was held constant using a Melcor thermoelectric cooler (TEC), typically at a temperature of 28.00°C. Both the TEC current and the laser injection current were supplied by a Profile laser diode combi controller (ITC-510). The injection current supply has a specification of being stable to 100 μA for 20 s, but performed better than this in practice. The output power was focused onto and detected using a fast photodiode (Alphalas UPD-40-VSI-P) with a rise time of less than 40 ps and a detection bandwidth of 12 GHz. This signal was captured by a 4-GHz-bandwidth digital sampling oscilloscope (DSO) (Agilent Infiniium 54854A) capable of capturing 20 GSa/s. The oscilloscope was set up to capture and average 1024 trigger events. A single RO has a detected amplitude of about 3 mV. The oscilloscope was operated at high sensitivity as the frequency of the signal was of the order of the bandwidth of the oscilloscope. In the prior work [3] the relaxation oscillation was analyzed by two methods—analyzing the time trace directly to calculate the frequency, and performing a fast Fourier transform (FFT) of the RO time trace using the inbuilt FFT tool of the DSO, and measuring the frequency of the RO peak. For the mid range of injection currents (48–58 mA) the uncertainty in the directly measured ROF was 0.3–0.5%, and 0.6–1.3% for the FFT generated values.

3 Instantaneous frequency measurement

The mathematics used in implementing the instantaneous frequency measurement is described briefly in the Appendix. It follows that presented in Refs. [6–10]. The concept of instantaneous frequency has been proposed as potentially allowing for the measurement of the frequency of a sub-one-oscillation signal [8]. The study herein allows discussion of this concept in the context of instantaneous frequency values of relaxation oscillations obtained. The steps involved in the instantaneous frequency measurement are: (i) creating an analytic signal from the real relaxation oscillation signal by calculating its Hilbert transform (which also requires the Cauchy principal value to be determined [9]) and adding 'i' times the Hilbert transform to the real signal [8] and (ii) applying an appropriate instantaneous frequency algorithm to the analytic signal to determine the IF. Several such algorithms are available and their comparative effectiveness when analyzing test signals, in terms of computational requirements and statistical variance, has been reported in [7]. The analysis included test signals with noise. The algorithms include the phase-difference estimator; zero-crossing method; moments and peaks of time–frequency distributions, like the Wigner–Ville distribution (WVD); and maximum-likelihood estimators [7]. The two algorithms used in analyzing the experimental relaxation oscillation frequency signals in this work are the phase-differencing estimator and the peak of the Wigner–Ville distribution. The phase differencing estimator algorithm gave values of the instantaneous frequency of the experimental relaxation oscillation data with unacceptably large uncertainties. The WVD gave very low statistical variance compared to other algorithms in [7], and the results obtained herein, with the WVD, had acceptable uncertainty. Only results using the WVD are reported. The WVD of the discrete time relaxation oscillation data was determined using a MATLAB program modified from one previously reported [10].

4 Results and discussion

Figure 1 illustrates the IFM analysis of a relaxation oscillation signal, for an injection current of 52 mA, using the WVD as the IF algorithm. The signal (top trace) was

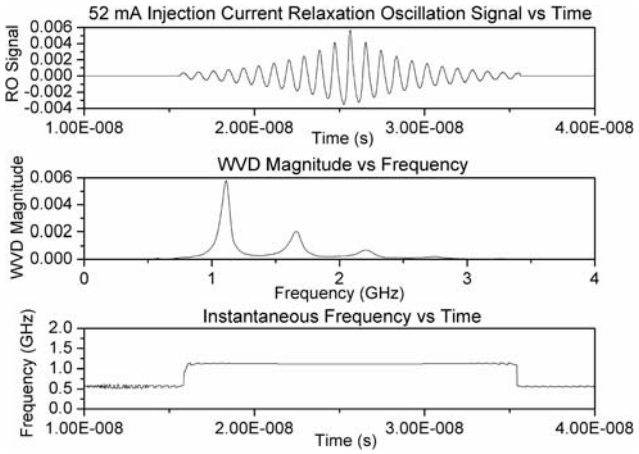

Fig. 1 Illustration of the IFM analysis: *top trace*—time average of 1024 relaxation oscillation events at an injection current of 52 mA; *mid trace*—single time slice of the magnitude of the WVD as a function of frequency; *lower trace*—IF as a function of time

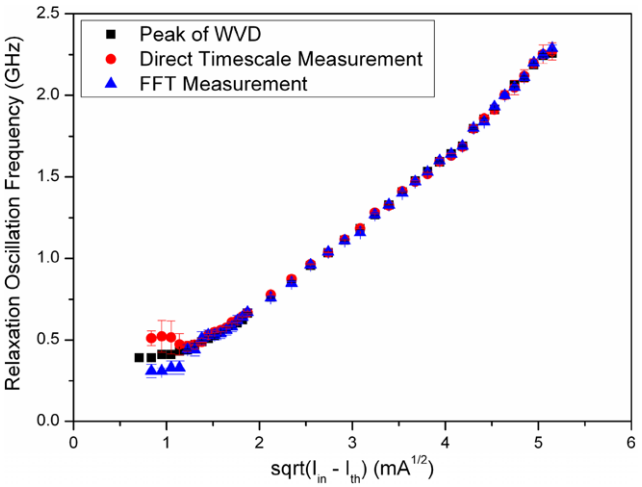

Fig. 2 Comparison of relaxation oscillation frequency as a function of square root of injection current above threshold, with the *error bars* showing the uncertainty in the ROF, obtained by IFM (*black squares*), with values obtained by direct time scale (*red circles*) and FFT (*blue triangles*) measurements

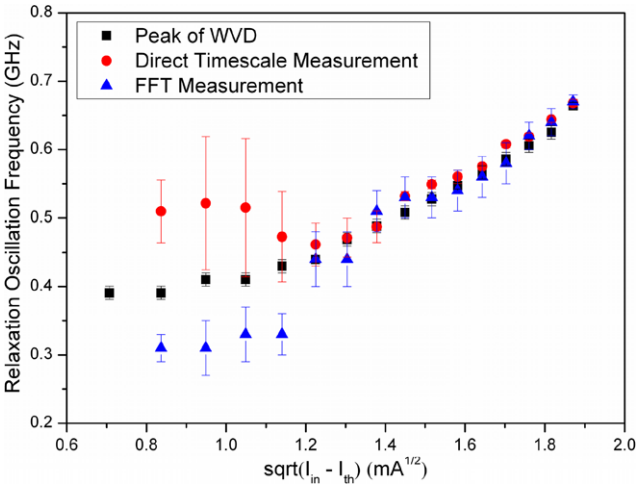

Fig. 3 Expansion of Fig. 2 to show that the IFM technique successfully extracts a weak oscillation of constant frequency, associated with the device packaging, circuitry and/or power supply, which dominates the variations in output power at injection currents close to threshold

zero padded to 6100 data points (see the Appendix) and the instantaneous frequency at the peak of the signal was 1.115 GHz (0.3%). The middle trace shows the magnitude of the WVD as a function of frequency for a single time and the bottom trace shows the peak value of the magnitude of the WVD for all times in the duration of the signal. The estimation from the direct time scale measurement was 1.117 GHz (0.3%) and from the peak of the FFT was 1.110 GHz (0.6%). The IF value obtained was constant across most of the duration of the relaxation oscillation event as shown in Fig. 1 (lower trace). Thus, this result supports the validity of the method in measuring the relaxation oscillation frequency of a laser.

The values obtained for the complete data set of relaxation oscillations is shown in Fig. 2. Comparison is shown with analysis by direct time scale and FFT methods [3]. The uncertainties in the values obtained using the peak of the WVD are smaller than for either direct time scale or FFT methods, as shown by the error bars in Fig. 2. Figure 3 shows the values obtained for low injection currents at higher resolution. Here it is seen that the IFM picks out a narrow bandwidth frequency oscillation at an approximately constant frequency (∼0.370 GHz) that dominates the detected signal at these low injection currents. Neither the direct time scale nor the FFT analysis led to recognition of this weak oscillation. Such an oscillation is readily linked to an oscillation excited by the cables, connectors and/or packaging. This allows a robust argument to be given as to why it is appropriate to exclude such data points from a graph of ROF versus square root of injection current above threshold when producing a line of best fit to the data. The IFM technique extracts additional information compared to the other analysis techniques that have been used.

The IFM values obtained at higher injection currents (60–70 mA) agree with values obtained by the direct time scale and FFT analysis methods and are consistently higher than expected from the theoretical dependency (1). The average of 1024 RO events at these injection currents can be less than one full period of oscillation and this is distorted by the impact of low-frequency oscillations (as for low injection currents). The results show there is no advantage gained in predicting the ROF using the IFM approach over the results previously obtained at high injection currents. The signal requirements for reliable IFM of very heavily damped sinusoidal oscillations have been systematically researched [11]. A more thorough exploration of the IFM signal processing of high-injection-current RO events has been possible [12]

using the results from [11]. It is concluded that it is not possible to extract meaningful ROF values by IFM at higher injection currents because the relaxation oscillation cannot be isolated from the total signal which is distorted by other high-frequency components. Use of an appropriate filter to reject the low-frequency components (<500 MHz) does not enable any extension of the upper bound of the range of injection currents for which RO events can be successfully captured and analyzed. It is necessary to have a relatively pure RO signal before analysis of the ROF by any technique is robust. This occurs for mid-range currents only.

ROF values from low and high injection currents that clearly do not show the expected linear dependency of ROF with square root of injection current above threshold are set aside as not being valid RO measurements. The IFM has given improved justification and understanding of why it is valid to set these values aside. The 'mid' injection current IFM ROFs have been used to determine the threshold current using the method reported previously [4]. This is done by extrapolation to zero ROF occurring at I_{th}, as described in [4]. The IFM-generated results using two RO data sets [3, 4], collected about sixteen months apart, are shown in Fig. 4. From the earlier data set (top graph) a value for I_{th} of (44.640 ± 0.005) mA is obtained. This compares with a value of 43.5 mA [3] using the two segment line fit method [5]. As shown in [4], the threshold current of a semiconductor laser tends to higher values as more precise methods for determining it are applied. Values of (44.550 ± 0.005) mA using direct time ROFs, and (44.700 ± 0.005) mA using the FFT ROFs, were obtained in this work using the data from [3]. The threshold current prediction from the WVD peak falls between the values obtained by the other two methods. It is more reliable than the other two, because of the smaller error bounds for the IFM RO estimations (Figs. 2 and 3). From the later data set a value of (44.970 ± 0.005) mA is obtained, as compared to (44.950 ± 0.005) mA in [4]. A small rise in threshold current (44.950 mA as compared to 44.640 mA), indicating an increase over the intervening 16 months, is likely to be real due to device aging.

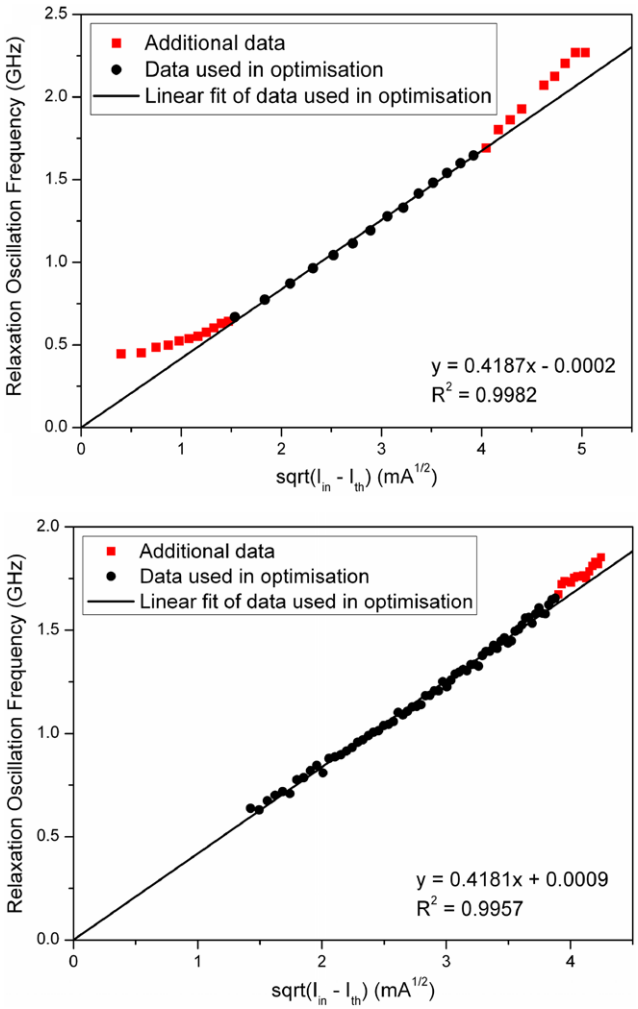

Fig. 4 Using the IFM-generated values of the relaxation oscillation frequency to show an excellent fit to the expected linear relationship with square root of injection current above threshold, when the fit uses a valid subset of the full data (*black circles*), but excludes data for which the value cannot be validated (*red squares*). The line of best possible fit in turn gives the most precise value for the threshold injection current for the semiconductor laser [4]. *Top graph* uses data from [3]. *Bottom graph* uses data from [4]

5 Conclusions

An instantaneous frequency measurement algorithm, using the Wigner–Ville distribution, has been developed, and applied successfully, to analyzing relaxation oscillation time signals from a semiconductor laser. Use of a phase-differencing estimator as the IF algorithm led to unacceptably large uncertainty in the IF value [11]. Using the WVD algorithm the uncertainty in the relaxation oscillation frequencies is at worst the same as that for direct time scale analysis, but elsewhere reduced by a factor of order two relative to the FFT method, developed and used previously [3, 4]. The relaxation oscillation frequencies obtained from IFM allow the threshold injection current to be determined with the same precision as using FFT values [4] but with increased reliability due to the reduced uncertainty in the ROF values.

Applying the IFM technique to averaged RO events at low (less than ∼5 mA above threshold) and high injection currents (more than ∼20 mA above threshold) does not lead to any improvement in extraction of the ROF. It does however lead to extraction of a dominant, constant low frequency oscillation associated with packaging, connections and powering of the device at low injection currents. The IFM of ROFs has given increased justification to the validity

of considering only ROFs obtained at mid-range injection currents in testing the validity of (1). It can be concluded that all the precision measurements of ROF show agreement with the dependency on injection current shown in (1), once injection currents for which it is not possible to obtain a valid ROF are excluded. Further testing and evaluation of the IFM technique applied to sub-one-period time signals is reported in [11].

Acknowledgements The authors would like to thank Josh Toomey for helpful discussions. This work was supported by the Australian Research Council as a part of a Discovery Project.

Appendix: Instantaneous frequency

In the conventional Fourier analysis of a signal, the frequency is defined for a sine or cosine function extending across the signal. With a definition of this type, the instantaneous frequency would necessarily correspond to the frequency of the sine or cosine function. At least a single oscillation is required to define the local frequency value. This definition is not applicable to non-stationary data in which the frequency occasionally changes. In this case a broader definition allowing for determination of the instantaneous frequency of signals with less than one full oscillation appears appropriate. The notion of instantaneous frequency has been proposed as perhaps allowing for the seemingly paradoxical measurement of the frequency of a sub-one-oscillation signal [8].

A The Hilbert transform

The instantaneous frequency is defined for analytic signals. The following, including (2)–(5), are reproduced from [8]. An analytic signal may be generated from a real one by using the Hilbert transform. Given a time series $X(t)$, its Hilbert transform $Y(t)$ is defined as

$$Y(t) = \frac{1}{\pi}(PV)\int_{-\infty}^{\infty} \frac{X(t')}{t-t'}\,\mathrm{d}t', \tag{2}$$

where PV represents the Cauchy principal value. The Hilbert transform is essentially the convolution of $X(t)$ with $1/t$. An analytic signal $Z(t)$ is formed from this complex conjugate pair,

$$Z(t) = X(t) + \mathrm{i}Y(t) = a(t)\mathrm{e}^{\mathrm{i}\phi(t)}, \tag{3}$$

where

$$a(t) = \left[X^2(t) + Y^2(t)\right]^{1/2} \tag{4a}$$

and

$$\phi(t) = \tan^{-1}\left(\frac{Y(t)}{X(t)}\right) \tag{4b}$$

are the amplitude and phase in polar coordinate form [8]. The polar coordinate expression fits an amplitude and phase varying trigonometric function to $X(t)$. The instantaneous frequency can then be defined as

$$\omega_\mathrm{i} = \frac{\mathrm{d}\phi(t)}{\mathrm{d}t}, \qquad f_\mathrm{i} = \frac{1}{2\pi}\frac{\mathrm{d}\phi(t)}{\mathrm{d}t}, \tag{5}$$

where ω_i is expressed in radians and f_i is in Hz.

B The Cauchy principal value

Let f be a function defined on the interval $I = [a, b]$, with $a < c < b$. Given that f is integrable on $[a, c-\delta]\cup[c+\delta, b]$ for all $\delta > 0$, the Cauchy principal value of

$$\int_a^b f(x)\,\mathrm{d}x \tag{6}$$

is defined as

$$(PV)\int_a^b f(x)\,\mathrm{d}x = \lim_{\delta\to 0}\left(\int_a^{c-\delta} f(x)\,\mathrm{d}x + \int_{c+\delta}^b f(x)\,\mathrm{d}x\right), \tag{7}$$

so that, if the integral exists, then the Cauchy principal value also exists and is equivalent to it. Alternatively, the integral may not exist while the Cauchy principal value does. The following integral diverges:

$$\int_a^b \frac{1}{x-c}\,\mathrm{d}x.$$

The Cauchy principal value is given by

$$\begin{aligned}
(PV)\int_a^b \frac{1}{x-c}\,\mathrm{d}x &= \lim_{\delta\to 0}\left(\int_a^{c-\delta}\frac{1}{x-c}\,\mathrm{d}x + \int_{c+\delta}^b \frac{1}{x-c}\,\mathrm{d}x\right)\\
&= \lim_{\delta\to 0}\left(\left[\ln|x-c|\right]_a^{c-\delta} + \left[\ln|x-c|\right]_{c+\delta}^b\right)\\
&= \lim_{\delta\to 0}\left(\ln|c-\delta-c| - \ln|a-c| + \ln|b-c|\right.\\
&\qquad \left. - \ln|c+\delta-c|\right)\\
&= \lim_{\delta\to 0}\left(\ln|-\delta| - \ln|a-c| + \ln|b-c| - \ln|\delta|\right)\\
&= \ln\left|\frac{b-c}{a-c}\right|,
\end{aligned}$$

which clearly does exist [9].

C Instantaneous frequency estimation algorithm—phase-differencing estimator

The simplest approach to making an instantaneous frequency estimate of a discrete-time signal is to use (5) to evaluate the derivative of the phase of the analytic signal with respect to time, $Z(t)$, associated with the real-time signal, $X(t)$. Differentiation can be carried out in discrete time using a discrete finite impulse response differentiator or by forward and backward finite phase differencing operations. Another method is the central finite difference (CFD) method, which is implemented in discrete time using the expression

$$f_c(n) = \frac{1}{2\pi} \frac{(\phi(n+1) - \phi(n-1))}{2\mathrm{d}t}, \tag{8}$$

where n is a particular element in a data set—an RO value for a unit of sampling time in the case herein. The advantages of this method over the other phase-differencing procedures are that it is unbiased and it also performs better with noisy signals than the finite impulse response method [7]. It was found that the variation in IF evaluated across the full time span of the signal being processed was unacceptably high with this method, both for ideal simulated signals and the experimental RO events.

D Instantaneous frequency estimation algorithm—the Wigner–Ville distribution

The peak of a periodogram or frequency spectrum is used as the estimate of the frequency of a stationary sinusoidal signal. This definition can be extended to non-stationary signals by estimating the IF of a signal at a discrete point in time from the peak of a time–frequency distribution. The Wigner–Ville distribution (WVD) is such a time–frequency distribution and one that is found to be noise tolerant [7].

The WVD is given in terms of the analytic signal $Z(t)$ by

$$W(t,\omega) = \frac{1}{2\pi} \int Z^*\left(t - \frac{1}{2}\tau\right) Z\left(t + \frac{1}{2}\tau\right) \mathrm{e}^{-\mathrm{i}\tau\omega}\, \mathrm{d}\tau, \tag{9}$$

where τ is an increment of time. The WVD at a time t is produced by adding the products of the signal at symmetrical points about t. If there is some correlation between the signal in the past and in the future then the properties of the signal at those times will exist at the present time, t. The Wigner distribution is non-local, as the signals at times distant from t are weighted equally to those close by. This non-locality leads to interesting properties, such as the Wigner distribution being non-zero at times when the signal is zero. It is also not strictly zero for frequencies that are not present in the spectrum. However, for finite-duration signals the Wigner distribution is zero before and after the signal starts and stops because the signal is zero in those domains [13]. It is advisable to zero pad the signal data set by extending the range of time over which a zero value is assigned. The longer the data set, the smaller the increment in the frequency vector, and the greater is the precision in estimating the IF.

The WVD of the discrete time relaxation oscillation data was determined using a MATLAB function based upon one reported in [10]. The function reads in a data vector, $Y(t)$ (which is the Hilbert transform of a real signal), and the sampling frequency of the signal, f_s. A time vector the same length as $Y(t)$ is generated from f_s. A frequency vector of the same length is also generated, which ranges between 0 Hz and $f_s/2$ Hz (the Nyquist frequency).

The instantaneous autocorrelation is calculated after generating a vector of discrete values of τ. The τ vector ranges between points in time such that when the signal is multiplied by the complex conjugate at some time lag, the time does not lie outside of the domain of the signal. An $N \times N$ matrix (where N is the length of $Y(t)$) of the discrete, instantaneous autocorrelations is produced, where τ increases down the columns and time increments through the rows. A Fourier transform is calculated for each column of the matrix, or the autocorrelation for each value of time. The matrix, and the time and frequency vectors, are then returned as the output. The matrix represents a two-dimensional function of time and frequency. The magnitude of the matrix is calculated, and the maximum value in each column is found. The maximum value is associated with a discrete frequency and time value, which leads to the IF relationship for the signal as a function of time. Figure 1 illustrates this for the analysis of an average of 1024 RO events, in the output power of a semiconductor laser, operated at a single injection current.

References

1. K. Petermann, *Laser Diode Modulation and Noise, Advances in Optoelectronics* (Kluwer, Dordrecht, 1988), p. 79
2. M. Hochholzer, W. Harth, IEE Proc. Optoelectron. **142**(5), 232 (1995)
3. C. McMahon, D.M. Kane, J.P. Toomey, J.S. Lawrence, in *Proc. Int. Conf. Nanoscience and Nanotechnology*, ed. by C. Jagadish, G.Q.M. Lu (IEEE, Brisbane, 2006), p. 497
4. D.M. Kane, J.P. Toomey, IEEE J. Lightwave Technol. **27**, 2949 (2009)
5. Bellcore standard *Introduction to Reliability of Laser Diodes and Modules*. Spec. Rep. SR-TSY-001369, available for purchase via http://telecom-info.telcordia.com/ido/AUX/SR_TSY_001369_TOC.i01.pdf
6. B. Boashash, Proc. IEEE **80**(4), 520 (1992)
7. B. Boashash, Proc. IEEE **80**(4), 540 (1992)

8. N.E. Huang, Z. Shen, S.R. Long, M.L.C. Wu, H.H. Shih, Q.N. Zheng, N.C. Yen, C.C. Tung, H.H. Liu, Proc. R. Soc. Lond. A, Math. Phys. Eng. Sci. **454**, 903(1998)
9. A. Zayed, *Handbook of Function and Generalized Function Transformations* (CRC, Boca Raton, 1996), p. 10
10. J.L. Semmlow, *Biosignal and Biomedical Image Processing MATLAB-Based Applications* (CRC, Boca Raton, 2004), p. 164
11. C. McMahon, D.M. Kane, Electron. Lett. (submitted)
12. C.J. McMahon, D.M. Kane, Accepted to *Int. Conf. Nanotechnology and Nanoscience (ICONN 2010)*, to be held at Sydney, Australia, 22–26 February 2010
13. L. Cohen, *Time–Frequency Analysis* (Prentice-Hall, New Jersey, 1995), p. 113